Advances in Radiation Oncology (2022) 7, 100942

advances in radiation oncology

www.advancesradonc.org

Scientific Article

Gadoxetic Acid Uptake Rate as a Measure of Global and Regional Liver Function as Compared With Indocyanine Green Retention, Albumin-Bilirubin Score, and Portal Venous Perfusion

Josiah Simeth, PhD,[a,b,c,*] Madhava Aryal, PhD,[a] Dawn Owen, MD, PhD,[d] Kyle Cuneo, MD,[a] Theodore S. Lawrence, MD, PhD,[a] and Yue Cao, PhD[a,b,e]

[a]Department of Radiation Oncology, University of Michigan, Ann Arbor, MI; [b]Biomedical Engineering, University of Michigan, Ann Arbor, MI; [c]Department of Medical Physics, Memorial Sloan Kettering, New York, NY; [d]Department of Radiation Oncology, Mayo Clinic, Rochester, MN; [e]Department of Radiology, University of Michigan, Ann Arbor, MI

Received August 25, 2021; accepted February 26, 2022

Abstract

Purpose: Global and regional liver function assessments are important for defining the magnitude and spatial distribution of dose to preserve functional liver parenchyma and reduce incidence of hepatotoxicity from radiation therapy for intrahepatic cancer treatment. This individualized liver function-guided radiation therapy strategy is critical for patients with heterogeneous and poor liver function, often observed in cirrhotic patients treated for hepatocellular carcinoma. This study aimed to validate k_1 as a measure of global and regional function through comparison with 2 well-regarded global function measures: indocyanine green retention (ICGR) and albumin-bilirubin (ALBI).

Methods and Materials: Seventy-nine dynamic gadoxetic acid enhanced magnetic resonance imaging scans were acquired in 40 patients with hepatocellular carcinoma in institutional review board approved prospective protocols. Portal venous perfusion (k_{pv}) was quantified from gadoxetic acid enhanced magnetic resonance imaging using a dual-input 2-compartment model, and gadoxetic acid uptake rate (k_1) was fitted using a linearized single-input 2-compartment model chosen for robust k_1 estimation. Four image-derived measures of global liver function were tested: (1) mean k_1 multiplied by liver volume (k_1V_L) (functional volume), (2) mean k_1 multiplied by blood distribution volume (k_1V_{dis}), (3) mean k_{pv}, and (4) liver volume (V_L). The measure's correlation with corresponding ICGR and ALBI tests was assessed using linear regression. Voxel-wise similarity between k_1 and k_{pv} was compared using Spearman ranked correlation.

Results: Significant correlations ($P < .05$) with ICGR and ALBI were found for k_1V_L, k_1V_{dis}, and V_L (in order of strength), but not for mean k_{pv}. The mean ranked correlation coefficient between k_1 and k_{pv} maps was 0.09. k_1 and k_{pv} maps were predominantly mismatched in patients with poor liver function.

Conclusions: The metric combining function and liver volume (k_1V_L) was a stronger measure of global liver function compared with perfusion or liver volume alone, especially in patients with poor liver function. Gadoxetic acid uptake rate is promising for both global and regional liver function.

Sources of support: This work was supported in part by NIH grants R01 CA132834 and P01 CA059827.

Disclosures: J.S. has patent 10010263 issued to University of Michigan.

Data sharing statement: Research data are not available at this time.

*Corresponding author: Josiah Simeth, PhD; E-mail: jjsimeth@umich.edu

https://doi.org/10.1016/j.adro.2022.100942

Introduction

Global liver function has been shown to be an important clinical prognostic factor for radiation induced liver disease and survival in patients with cirrhosis and hepatic cancers.[1-4] Liver injury during radiation therapy (RT) of hepatic cancers has been minimized using normal tissue complication probability models by limiting mean liver dose.[1,2,5] Individualized adaptive RT strategies have been suggested and investigated to further minimize risks of liver injury. Using this strategy, separate patients cannot be assumed to have the uniform liver function and radiation dose response. Furthermore, a patient cannot be assumed to have homogeneous hepatic function and dose-response throughout the liver.[6-10] These approaches require measures of global and regional liver function as well as radiation dose response in individual patients while considering all these factors in treatment planning.

Various measures have been used as surrogates for regional liver function. Vascular contrast agents, such as gadobenic acid, have enabled interrogation of portal venous perfusion through dynamic gadobenic acid enhanced magnetic resonance imaging (MRI) scans of the liver.[11-13] Portal venous perfusion is significantly correlated with overall function evaluated via indocyanine green (ICG) clearance.[11,14,15] However, perfusion, whether arterial, venous, or total, is an indirect analog to liver function. Hepatobiliary contrast agents, such as gadoxetic acid, are taken up by the hepatocytes themselves, and quantification of this uptake rate can be used as a more direct measure of liver function.[12,16-19] These hepatobiliary agents enable quantification of both perfusion and uptake through a dual-input, 2 compartment (DITC) model of contrast kinetics.[16] Though the DITC model estimates perfusion and uptake parameters, the analysis requires an intensive fitting process over 6 parameters, which is highly susceptible to overfitting. Alternatively, the uptake parameters can be derived from a more robust linearized single-input 2 compartment (LSITC) model of gadoxetic acid uptake rate.[17] There are parallel capacities in other modalities. For instance, iminodiacetic acid (IDA) single photon emmision coherence tomography (SPECT)[7,20] shares similar hepatocellular uptake characteristics to gadoxetic acid, though gadoxetic acid benefits from superior spatial and temporal resolutions and soft tissue contrast in MRI. Similar advantages have motivated MRI guided RT.[21,22]

We hypothesized that global and regional liver function can be quantified from a single measure using gadoxetic acid uptake rate (k_1) derived by fitting dynamic MRI to LSITC. This study aimed to validate k_1 as a measure of global and regional function by comparison with 2 established global function measures, ICG retention at 15 minutes (ICGR15) and raw albumin-bilirubin (ALBI) score.[23] Uptake was compared with portal venous perfusion (k_{pv}) in relation to total function and spatial distribution.

Methods and Materials

Models

Hepatic perfusion and uptake rate can be estimated using the DITC model of gadoxetic acid dynamics.[16,17] Contrast concentration in a liver volume of interest V_t consists of components in the extracellular and intracellular spaces:

$$\overbrace{V_t C_t(t)}^{Contrast\ in\ Tissue} = \overbrace{V_{dis} C_{dis}(t)}^{Extracellular\ Contrast} + \overbrace{k_1 \int_0^t V_{dis} C_{dis}(\tau) d\tau}^{Intracellular\ Contrast} \quad (1)$$

$$V_{dis} C_{dis}(t) = V_{dis} \int_0^t \left(k_a C_a(\tau - \tau_a) + k_{pv} C_{pv}(\tau - \tau_{pv}) \right) e^{-(t-\tau)(k_2 + k_1)} d\tau \quad (2)$$

where V_{dis} is the distribution volume of blood; C_t, C_{dis}, C_a, and C_{pv} are contrast concentrations as a function of time in the respective total, distribution, arterial blood, and portal venous blood volumes; τ_a and τ_{pv} describe respective arrival time delays of the arterial and portal vein input functions at each voxel; k_a and k_{pv} describe the normalized arterial and portal venous flow rates; and k_2 is the hepatic perfusion, defined as the normalized flow rate leaving the volume of interest through the central vein. k_1 is the normalized rate of uptake of contrast to the intracellular space. The distribution volume includes the space of Disse and sinusoids.[16] A nonlinear least squares (NLLS) fitting of this model to measured C_t based on measured C_a and C_{pv} input functions yields estimates of k_a, k_{pv}, k_1, k_2, V_{dis}, τ_a, and τ_{pv}.

To estimate k_1 alone, the computationally simpler LSITC model can yield more robust estimation than the DITC model.[17] Detailed derivation and fitting of the LSITC model are given in reference 17. In brief, the LSITC model is given by:

$$\overbrace{\frac{(1 - Hct) C_t(t)}{C_a(t)}}^{y} = \overbrace{v_{dis} k_1}^{slope} \overbrace{\frac{\int_0^t C_a(\tau) d\tau}{C_a(t)}}^{x} + \overbrace{v_{dis}}^{intercept} \qquad t > t_0 \quad (3)$$

Note that k_1 can be calculated by a ratio of slope to intercept obtained from a linear least squares fitting of equation 3 for temporal data after t_0. Model assumptions and derivation of t_0 are fully described in reference 17. Briefly, t_0 is determined by analysis of data linearity following equation 3 using principal component analysis.

Data acquisition

Patients

Seventy-eight dynamic gadoxetic-acid enhanced (DGAE) liver MRI scans were acquired from 40 patients (median age of 64 years) with liver cancer in prospective

Table 1 Patient demographics for all 40 patients

Characteristic	Value
Age (years): Median (range)	64 (48-100)
Sex: Female/male	9/31
Pretreatment cirrhosis (%)	82.5 (33 of 40)
HCC (%)	85.0 (34 of 40)
Liver volume (L): Median (range)	1.80 (0.69-3.99)
GTV volume (mL): Median (range)	43 (2.7-1251)
Child-Pugh score: Median (range)	6 (5-10)
Raw ALBI score (n = 37)	
Pre-RT: Median (range)	−2.2 (−3.6 to −1.0)
Post-RT: Median (range)	−2.0 (−3.27 to −1.0)
ICGR15 (%) (n = 35)	
Pre-RT: Median (range)	29.2 (4.0-82.3)
Post-RT: Median (range)	40.6 (7.5-82.3)

Abbreviations: ALBI = albumin-bilirubin; GTV = gross tumor volume; HCC = hepatocellular carcinoma; ICGR15 = indocyanine green retention at 15 minutes; RT = radiation therapy.

protocols approved by the University of Michigan institutional review board. All patients signed written consent forms. The patient demographic information is given in Table 1. Liver DGAE MRI scans were obtained pre-RT and 1 month post-RT. In all but 4 cases the ICG retention examination (a total liver function measure) was taken within 1 week of the MRI scans. In total, 69 pairs of DGAE MRI scans and ICG retention scores were available for correlation analysis of global liver function.

Image acquisition

Three-dimensional volumetric DGAE MRI scans of the whole liver were acquired using a radial sampling VIBE sequence during intravenous injection of a single standard dose of gadoxetic acid on a 3T scanner (Skyra, Siemens Healthineer). DGAE scans were acquired with a flip angle of ∼13.5°, echo time of ∼1.18 ms, and repetition time of 2.81 ms. The field of view was ∼420 mm, with an in-plane resolution of ∼2.19 × 2.19 mm for 64 slices with a slice thickness of ∼3.5 mm. The free-breathing DGAE images of the liver used a 3-dimensional golden-angle radial stack-of-stars volumetric interpolated breath-hold examination (VIBE) sequence that oversamples the center of k-space and is resilient to motion effects.[24] Acquisitions included image volumes from before contrast introduction to 4 to 31 minutes after the initial arterial peak (median 18 minutes). Dynamic image volumes of the whole liver were reconstructed with a temporal sampling rate of 3.4 to 15.2 seconds per volume (median, 8.8 seconds), 64 to 80 slices with thicknesses from 2.6 to 4.8 mm, and an in-plane resolution of 2.1 × 2.1 to 2.6 × 2.6 mm (192 × 192 pixels).

ICG retention test

ICG retention examinations used a single dose of ICG with blood sampled at 5, 10, and 15 minutes after injection to measure the fractional retention of ICG. ICG is cleared almost entirely in the liver,[25] making measures of ICG clearance a common surrogate for global liver function.[6] See reference 10 for a more in-depth description of the ICGR15 procedure.

ALBI

The ALBI score was computed using serum bilirubin and albumin levels using the equation given by Johnson et al[23]:

$$\mathrm{ALBI} = \left(\log_{10}(\mathrm{bilirubin}) \times 0.66\right) + (\mathrm{albumin} \times -0.085) \tag{4}$$

with bilirubin in μmol/L and albumin in g/L. Though this score can be used to rate the patient's global liver function with a discrete ALBI grade, the raw ALBI score is a continuous measure.

Image processing and analysis

Image preprocess and model fitting

The time-series DGAE-MRI volumes were coregistered within the liver contour using an overdetermined, rigid-body transformation approach.[15] Then, both DITC and LSITC models were applied to the registered time-series DGAE-MRI volumes to estimate $k_{pv,}$ $\mathrm{k_1}$, *and* $\mathrm{v_{dis}}$ using respective NLLS and linear least squares (LLS) fitting implemented in Matlab.

Similarity between perfusion and uptake rate maps

To assess portal venous perfusion (k_{pv}) as a surrogate for liver function, the correspondence between uptake rate (k_1) and k_{pv} was investigated using the ranked Spearman correlation. Correlations were considered significant when a correlation of zero was outside the 95% confidence interval (this is equivalent to setting $P < .05$ as the significance threshold). Both k_{pv} and k_1 maps were obtained from NLLS fitting of the DITC model. To exclude vasculature from the evaluation, all regions with a blood distribution volume (v_{dis}) > 0.25 were omitted from comparison.

Global liver function measures derived from imaging

There are several plausible ways of constructing a global measure of liver function from imaging. (1) A simple measure could be the mean k_{pv} ($\overline{k}_{\mathrm{pv}}$) in the liver.[11] (2) A total functional volume would be calculated by incorporating the

liver volume with the uptake rate (k_1) as a sum of k_1V_t across the liver or equivalently mean k_1 by total volume ($\overline{k}_1V_L$). (3) A prior study suggested that the blood distribution volume that provides the surface area for the gadoxetic acid uptake by parenchyma might be considered in the functional volume computation instead of using the absolute liver volume.[17] This measure would be expected to correspond to the total rate of gadoxetic acid uptake as a sum of $K_1 = k_1 \times V_{dis}$. (4) Finally, a total liver volume, which is a conventional measure used in liver resection,[26] could be included for comparison. All 4 imaging- derived candidates of global liver function measures were tested by a linear regression with ICGR15 and ALBI score.[23] These linear regressions also serve as a calibration measure to compute global liver function from DGAE MRI. Because the rate of ICG clearance is proportional to the log of ICG retention, a linear relationship would be expected between the log of ICGR15 and a measure of liver function.

The initial 3 tested global liver function measures: (1) mean k_{pv}, (2) mean k_1 × total volume (mL/min) (ie, $\overline{k}_1V_L$), and (3) summed K_1 were calculated in the contoured liver volume with uptake rates > 0 mL/100mL/min and distribution volumes $0.02 < v_{dis} < 0.25$ to exclude the liver contour variation and blood vessel. The volume-based measure included the entire contoured liver volume minus the gross tumor volume. Because some measures (2,3,4) are based on a totaled capacity, each measure was also compared with ICGR15 and ALBI score after normalization by patient mass.

Results

Similarity between perfusion and uptake rate maps

Portal venous perfusion and uptake rate varied greatly between patients and within patients. Example slices of k_1 and k_{pv} maps of 4 patients with different ICGR15 scores are shown Figure 1. Note that the differences were extreme in some patients, especially those with very poor liver function. The second left column in Figure 1 shows that a patient with ICGR15 and ALBI of 82.3% and -1.29 had a negative correlation of -0.34 due to negligible uptake rate of gadoxetic acid throughout the majority of the liver but relatively healthy perfusion through the liver.

In 26 of the 79 DGAC MRI scans, k_{pv} maps had extremely low values with local variation resembling noise. In these cases we observed a mean $k_{pv} < 0.005$ mL/min/(100 mL), but typically much lower, compared with typical values of 10 to 60 mL/min/(100 mL) from other patients. It is conceivable that this was caused by the existence of cirrhosis and hepatocellular carcinoma (HCC) in the patients or, more likely, by unreliable estimation of k_{pv} in the cases with poor hepatic perfusion using 1 standard dose of gadoxetic acid (in which Gd counts are one-quarter of the counts in 1 standard dose of Gadopentetic acid) and using the DITC model. To make the comparison fair, the 26 instances with negligible perfusion were

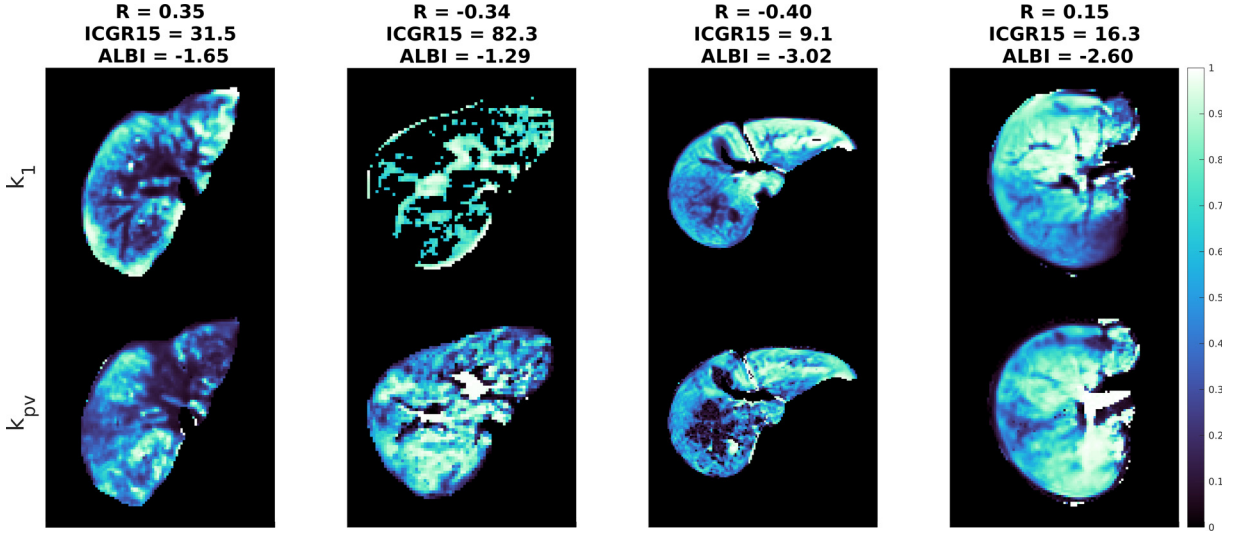

Figure 1 Example slices of k_1 (top row) and k_{pv} maps (bottom row) presented in 100 quantiles of 4 patients with different indocyanine green retention at 15 minutes (ICGR15) and albumin-bilirubin (ALBI) values. Note that large vessels generally show as dark in uptake rate maps (lacking hepatocytes), while in perfusion maps they can be either dark (arterial vessels) or bright (portal venous vasculature), depending on the type of vessels. The first patient shows a weak but nonnegligible correlation. The second depicts a patient, where despite severely compromised liver function observed by ICGR, ALBI, and negligible uptake rate throughout the liver, the perfusion is relatively uncompromised. The third and fourth patients have relatively good function, but still negligible to negative correlations in terms of uptake rate and perfusion, because the regional variations often do not match.

excluded from the analysis of the correlation between k_{pv} and k_1.

In the remaining 53 examinations, the correlation was still poor on average. The mean ranked correlation between uptake rate and perfusion maps was R = 0.095 (median, 0.12; range, −0.45 to 0.56). Figure 2 shows the distribution of ranked correlations between k_1 and k_{pv} values. Note that there were only 2 examinations that showed a positive correlation greater than 0.4. Between a third and one-half of the examinations had negative or near zero correlation between k_1 and k_{pv} in the liver, indicating a mismatch or nonmatch between hepatic perfusion and liver function.

Imaging-derived measures of total liver function compared with ICG and ALBI

Perfusion-derived measure

The correlation between mean k_{pv} and both $\log_{10}$(-ICGR15) and ALBI was poor. Twenty-three examinations were removed from the correlation analysis due to a failure in fitting k_{pv}, as seen by extremely low k_{pv} values across the liver volume. In these 23 examinations, there were no voxels that had k_{pv} values greater than 0.6 mL/(100 mL min) and less than 300 mL/(100 mL min) (artifacts). Without these 2 limits in place the fit was dominated by extreme outliers. As seen in Figures 3d and 4d and Table 2, there was not a significant correlation between mean portal venous perfusion and ICGR15 or ALBI (R = 0.03 and R = 0.06).

Uptake-derived measures

The total functional volume, quantified by the product of the mean k_1 in the liver and the total liver volume (determined using the LSITC model), had a strong correlation with both ICGR15 and ALBI (R = −0.67 and R = −0.73, respectively; see Fig. 3a and 4a). To calibrate the total functional volume against ICGR15, a linear regression model was tested after the removal of an outlier (k_1 > 3 median absolute deviations from the median; see Table 2). Normalization by patient mass resulted in strengthened correlations (R = −0.76 and R = −0.75 for ICGR15 and ALBI, respectively), with the corresponding fits given in Table 2.

The summed K_1 (accounting for the total blood distribution volume instead of the total liver volume) correlated well with ICGR15 and ALBI (R = −0.61 and R = −0.71) but was weaker than expected for ICGR15 based on preliminary studies[17] or the apparent analogy between total K_1 and ICG uptake rate. There appeared to be approximately 10 examinations that had $\log_{10}$(-ICGR15) values near 1 but had a systematic deviation from the regression line (see Fig 3b). This pattern was not seen in the corresponding ALBI scores. The linear regression models are given in Table 2. Normalization by patient mass again resulted in strengthened correlations (R = −0.69 and R = −0.74).

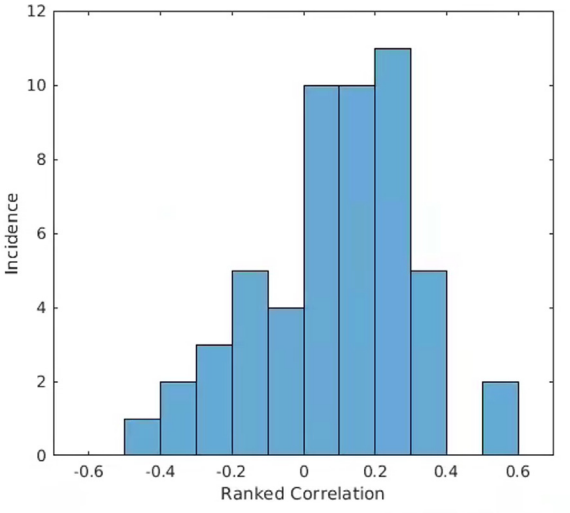

Figure 2 Histogram of the distribution of ranked correlations between k_1 and k_{pv} values (mean, 0.095; median, 0.12; n = 53).

Volume-derived measure

Liver volume showed a moderate correlation with $\log_{10}$(ICGR15) (R = −0.30), which was similar to preexisting studies[27-29] (see Fig 3d and Table 2), and comparable correlations for ALBI (R = −0.40) (see Fig 4d and Table 2). Only the ICGR15 correlation was strengthened by normalization by patient mass (R = −0.39). The correlation for mass normalized liver volume and ALBI showed an apparent strengthening of the linearity of the relationship for most points but created several outliers that canceled out this effect (R = −0.40).

Discussion

This study evaluated 4 potential measures of liver function from a single imaging measurement against 2 well-regarded measures of global liver function. The analysis shows that the total functional volume quantified by fitting LSITC to the DGAE-MRI, which accounts for both liver volume and gadoxetic acid uptake rate, is a better measure for global liver function than mean portal venous perfusion or liver volume, especially in the patients with a mis-match between hepatic perfusion and functional parenchyma. This single imaging technique can be used for measures of both global and regional liver function and can aid in liver function preservation during adaptive RT of hepatic cancers.

The results of this analysis underscore the differences between total functional volume and liver volume. The conventional normal tissue complication probability models, although providing guidance for radiation dose

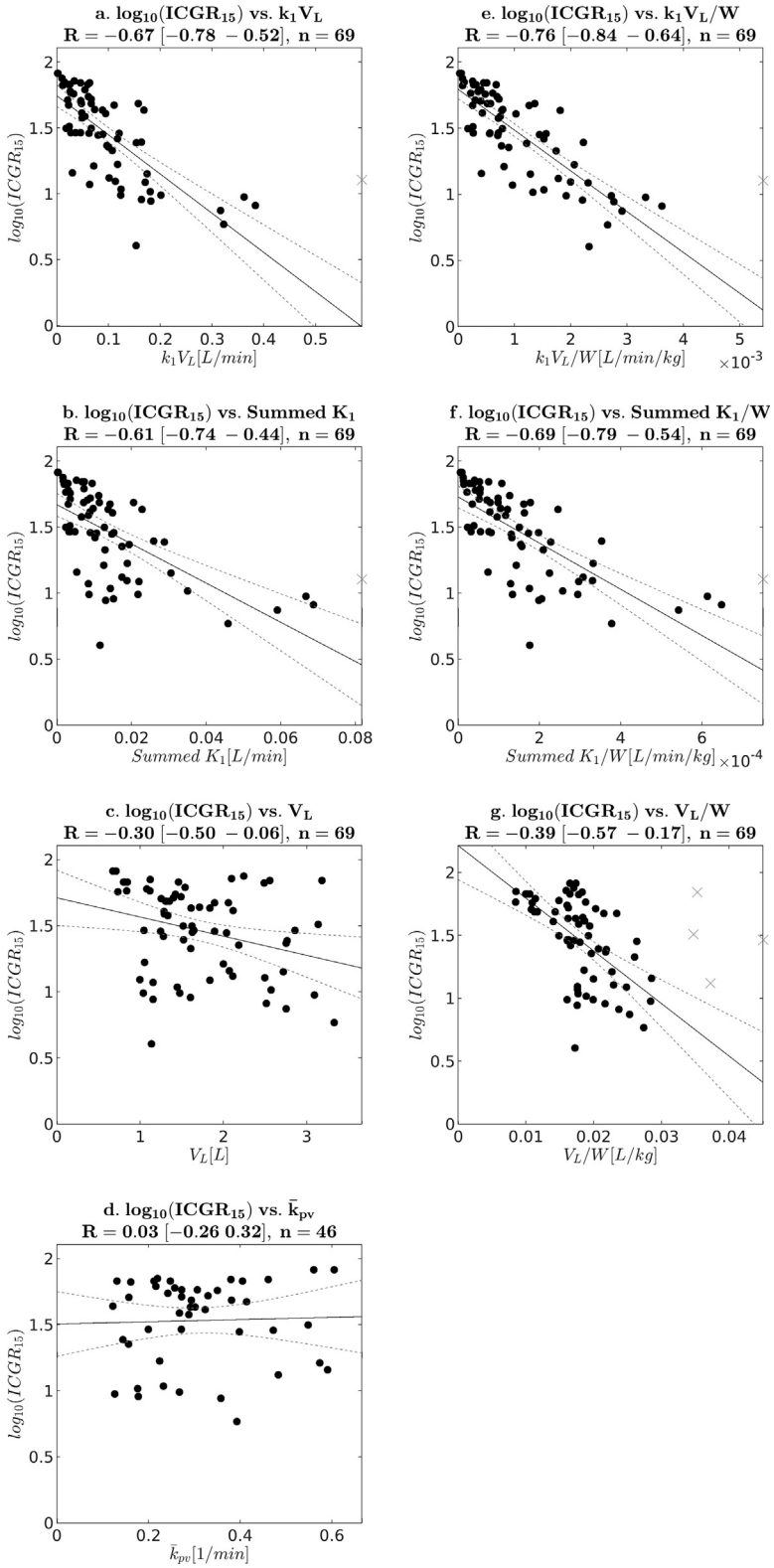

Figure 3 Log_{10} indocyanine green retention at 15 minutes (ICGR15) plotted against: (a) mean k_1 by total volume, (b) summed K_1 = summed k_1V_{dis}, (c) total liver volume outside gross tumor volume (GTV), (d) mean k_{pv}, (e) weight (W)-normalized mean k_1 by total volume, (f) W-normalized summed K_1 = summed k_1V_{dis}, (g) W-normalized total liver volume outside GTV. The plotted linear regression fit in (a), (b), (e), and (f) each ignore 1 outlier in terms of k_1, and the fit for (g) ignores 4 outliers in terms of W-normalized liver volume. Correlation coefficients do not exclude outliers.

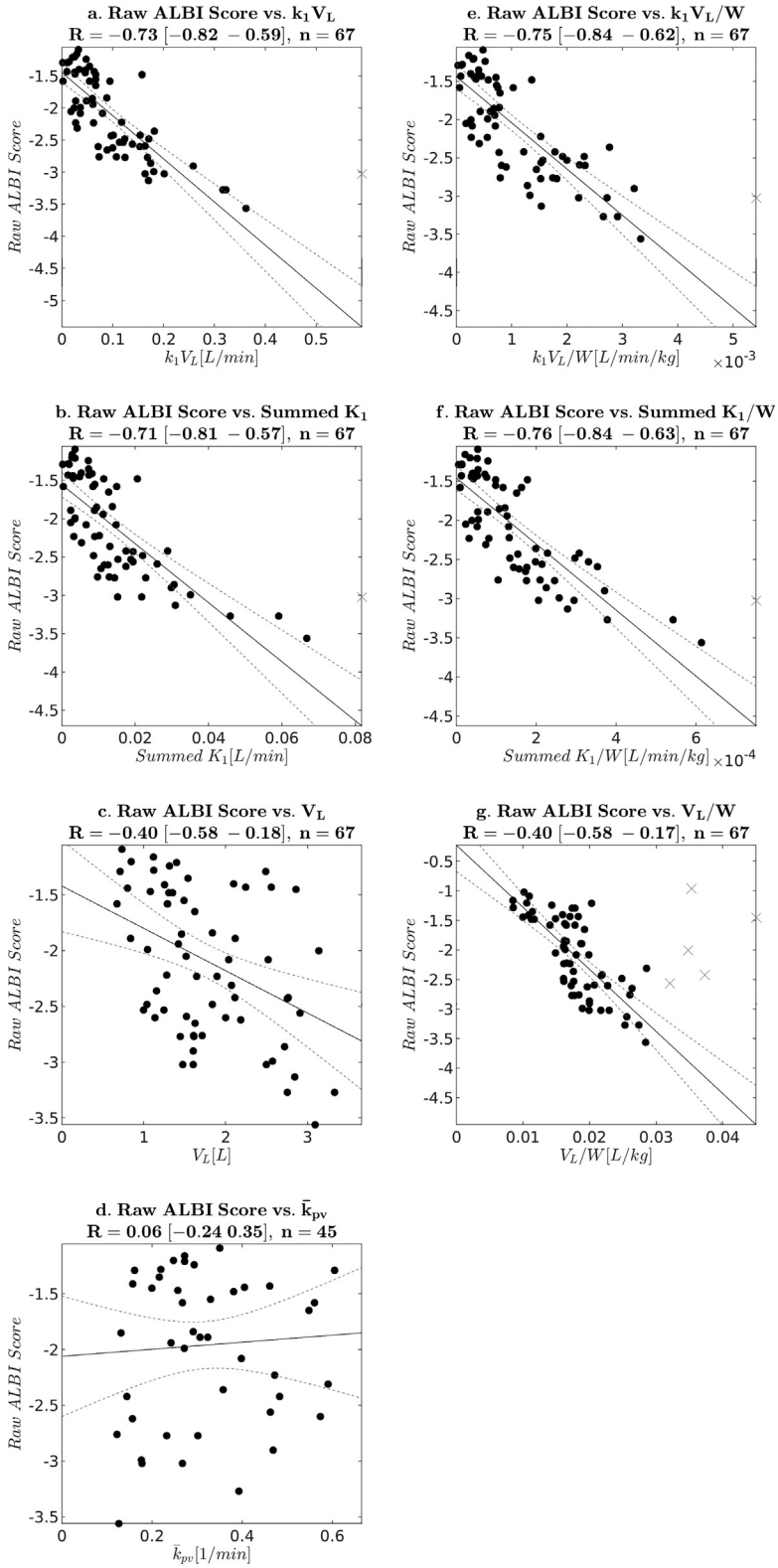

Figure 4 The raw albumin-bilirubin (ALBI) plotted against: (a) mean k_1 by total volume, (b) summed K_1 = summed k_1V_{dis}, (c) total liver volume outside gross tumor volume (GTV), (d) mean $k_{pv,}$ (e) weight-normalized mean k_1 by total volume, (f) weight-normalized summed K_1 = summed k_1V_{dis}, (g) weight-normalized total liver volume outside GTV. The plotted linear regression fit in (a), (b), (e), and (f) each ignore 1 outlier in terms of k_1, and the fit for (g) ignores 5 outliers in terms of weight-normalized liver volume. Correlation coefficients do not exclude outliers.

Table 2 Linear regression models of imaging-derived total liver function measures to ICGR15 and ALBI

Measure used to predict $\log_{10}$(ICGR15)	R	Slope (95% CI)	Intercept (95% CI)
$\overline{k}_{pv}$ [/s]	0.03	0.0838 (−0.64 to 0.81)	1.51 (1.26-1.75)
$\overline{k}_1 V_L$ [L/min]	−0.67	−2.97 (−3.63 to −2.31)	1.74 (1.66-1.83)
$\overline{k}_1 V_L$/W [L/min/kg]	−0.76	−308.5 (−362.6 to −254.6)	1.79 (1.72-1.87)
Summed K_1 [L/min]	−0.61	−14.85 (−19.29 to −10.40)	1.67 (1.58-1.76)
Summed K_1/W [L/min/kg]	−0.69	−1749 (−2167 to −1330)	1.73 (1.64-1.81)
V_L [L]	−0.30	−0.145 (−0.26 to −0.03)	1.71 (1.50-1.92)
V_L/W [L/kg]	−0.39	41.84 (−56.44 to −27.24)	2.21 (1.94-2.48)
Measure used to predict ALBI	R	Slope (95% CI)	Intercept (95% CI)
$\overline{k}_{pv}$ [/s]	0.06	0.3155 (−1.25 to 1.88)	−2.06 (−2.60 to −1.52)
$\overline{k}_1 V_L$ [L/min]	−0.73	−6.7242 (−8.00 to −5.45)	−1.45 (−1.60 to −1.29)
$\overline{k}_1 V_L$/W [L/min/kg]	−0.75	−604.7 (−723.3 to −486.1)	−1.44 (−1.60 to −1.28)
Summed K_1 [L/min]	−0.71	−38.50 (−47.07 to −29.94)	−1.56 (−1.72 to −1.40)
Summed K_1/W [L/min/kg]	−0.76	−4215 (−5027 to −3403)	−1.46 (−1.62 to −1.30)
V_L [L]	−0.40	−0.38 (−0.59 to −0.16)	−1.42 (−1.83 to −1.01)
V_L/W [L/kg]	−0.40	−105.1 (−129.2 to −81.11)	−0.23 (−0.67 to 0.22)

Abbreviations: ALBI = albumin-bilirubin; CI = confidence interval; ICGR15 = indocyanine green retention at 15 minutes.
Least-squared fitting of the global measures (log[ICGR15] or ALBI) from the given measure using the equation: global measure = slope × measure + intercept. The fits ignore the outliers marked in Figures 3 and 4. W represents the patient weight.

planning and avoiding liver injury, assume uniform hepatic function distribution over the liver volume.[5,30,31] Although in most metastatic cases liver function is likely uncompromised outside the region of the tumor, this is not the case for patients with primary liver cancer. Not considering function distribution in the liver volume could risk overestimation of liver function. As previously mentioned, patients treated for HCC are likely to have preexisting cirrhosis, resulting in significant compromise to liver function outside regions directly affected by the tumor. In this study, we showed that liver volume was poorly correlated with total function measured by ICG or ALBI, which was similar to prior studies,[27-29] suggesting liver volume is a poor marker for liver function. Therefore, a measurement of the regional hepatic function needs to consider more than liver volume alone.

MRI and SPECT imaging techniques have been used to measure spatially resolved liver function.[20,32] DGAE MRI scans allow assessments of hepatocyte function through contrast uptake, rather than assuming uniform function or interrogating the "plumbing" of the liver as in perfusion studies. Quantitative assessment of the extent of function in the regional units (voxels) allows one to compute a sum of the function of units as a measure of global liver function. Various models can determine uptake rate (eg, DITC, LSITC, DITC with bidirectional exchange or efflux terms). The robustness of these models is critical in ensuring a well-informed treatment plan for every patient. Although we initially predicted summed volumetric uptake rate would correlate well with global function, a stronger correlation was found for $k_1 V_L$ than for $k_1 V_{dis}$. Both uptake-based measures benefited from normalization by patient weight, particularly compared with ICGR15.

Other quantitative or semiquantitative methods have been used to derive metrics from DGAE MRI, for example, hepatic extraction fraction, liver-to-spleen ratio, and hepatocyte transport indices. Hepatic extraction fraction and liver-to-spleen ratio, although showing promise in prediction of global liver function in patients with good liver function,[27-29,33,34] do not differentiate contrast uptake by parenchyma from contrast in blood plasma, and the latter assumes conformity to flow enhancement in the spleen. Although semiquantitative measures benefit from simplicity, they are more scanner- and acquisition-dependent measures.[35] Another study performed a volume of interest based uptake rate calculation using static gadoxetic acid enhanced images and T1 relaxometry during hepatobiliary phase.[36] The volume-based uptake rate calculation does not account for the spatial contribution of hepatic function and cannot provide regional liver functional distribution to guide RT planning. The LSITC model can overcome these challenges and is less sensitive to temporal resolution of dynamic scans and arterial input function, providing robust voxel-by-voxel estimation in the gadoxetic acid uptake rate.

Previous work has shown strong correlation between global function and mean perfusion.[11,15] However, these

studies have had relatively small sample populations with higher liver function and lower rates of HCC and cirrhosis compared with this study. These studies found linear correlations of 0.70 (17 patients) and 0.92 (9 patients) between ICG rates and mean global k_{pv}, but had a lower representation of patients with HCC, and, predictably, lower rates of respective pretreatment cirrhosis, 35% and 11%, compared with 83% in the present study. A similar reality can be observed in ICGR15, where the 2 prior studies had respective ICGR15 ranges of 6.72% to 53.18% and 9.92% to 34.43%, compared with 4.04% to 82.3% in this study. Although cirrhosis does result in compromised portal venous perfusion,[37] that doesn't necessarily indicate that the level of functional compromise is predictable via the level of compromise in perfusion. The presence of high perfusion in these regions does not indicate healthy uptake. Correspondingly, it is possible for losses in functional hepatocytes to be mismatched from restricted perfusion as disease progresses (see the second column of Fig 1). Wang et al[14] used portal venous perfusion to create functional probability maps, with good correlation to ICG rates. However, their analysis showed increased uncertainty for patients with HCC, which is consistent with the failure in this study to replicate the strong correlations found between ICG retention rates and mean perfusion in healthier, noncirrhotic patient populations. Added to the findings of Wang et al, the results of this study indicate that perfusion is not a reliable indicator of function in populations with poor liver function and cirrhosis.

There are limitations in fitting the DITC model, including both perfusion and contrast uptake rate from DGAE MRI, which requires more precise temporal characterization of the portal venous and arterial input functions. Many examinations were not successfully fit via the DITC model, which is unsurprising given its complexity. We should particularly expect difficulty in differentiating k_a and k_{pv} when C_a and C_{pv} are very similar. In cases where perfusion is the desired measure, gadoxetic acid is the preferred contrast, but because it is not a hepatobiliary contrast agent, it precludes derivation of uptake rate. Use of gadoxetic acid in this instance allowed for direct comparison in a single scan without registration considerations and is justified when regional liver function is the desired measure. If the gadoxetic acid uptake rate is the primary interest, LSITC provides more robust estimation.

Conclusions

Gadoxetic uptake is promising in regional and global estimation of liver function, including "functional reserve." This is especially relevant when liver function is highly compromised and heterogeneous, where the uptake-based measures are most reliable.

Acknowledgments

The authors thank Siemens Healthineer for providing the Radial VIBE pulse sequence.

References

1. Koay EJ, Owen D, Das P. Radiation-induced liver disease and modern radiotherapy. *Sem Radiat Oncol*. 2018;28:321–331.
2. Suresh K, Owen D, Bazzi L, et al. Using indocyanine green extraction to predict liver function after stereotactic body radiation therapy for hepatocellular carcinoma. *Int J Radiat Oncol Biol Phys*. 2018;100:131–137.
3. Yoon HI, Koom WS, Lee IJ, et al. The significance of ICG-R15 in predicting hepatic toxicity in patients receiving radiotherapy for hepatocellular carcinoma. *Liver Int*. 2012;32:1165–1171.
4. Oellerich M, Burdelski M, Lautz HU, Binder L, Pichlmayr R. Predictors of one-year pretransplant survival in patients with cirrhosis. *Hepatology*. 1991;14:1029–1034.
5. Dawson LA, Normolle D, Balter JM, McGinn CJ, Lawrence TS, Ten Haken RK. Analysis of radiation-induced liver disease using the Lyman NTCP model. *Int J Radiat Oncol Biol Phys*. 2002;53:810–821.
6. Reeder SB. Quantification of liver function with MRI: Is it ready? *Radiology*. 2018;290:134–135.
7. Bennink RJ, Cieslak KP, van Delden OM, et al. Monitoring of total and regional liver function after SIRT. *Front Oncol*. 2014;4.
8. Wu VW, Epelman MA, Wang H, et al. Optimizing global liver function in radiation therapy treatment planning. *Phys Med Biol*. 2016;61:6465–6484.
9. Ge PL, Du SD, Mao YL. Advances in preoperative assessment of liver function. *Hepatobiliary Pancreat Dis Int*. 2014;13:361–370.
10. Stenmark MH, Cao Y, Wang H, et al. Estimating functional liver reserve following hepatic irradiation: Adaptive normal tissue response models. *Radiother Oncol*. 2014;111:418–423.
11. Cao Y, Wang H, Johnson TD, et al. Prediction of liver function by using magnetic resonance-based portal venous perfusion imaging. *Int J Radiat Oncol Biol Phys*. 2013;85:258–263.
12. Yamada A. Quantitative evaluation of liver function within MR imaging. In: El-Baz AS, Saba L, Suri J, eds. *Abdomen and Thoracic Imaging*. New York: Springer; 2014:233–251.
13. Sourbron SP, Buckley DL. Tracer kinetic modeling in MRI: Estimating perfusion and capillary permeability. *Phys Med Biol*. 2012;57:R1–33.
14. Wang H, Feng M, Jackson A, Ten Haken RK, Lawrence TS, Cao Y. A local and global function model of the liver. *Int J Radiat Oncol Biol Phys*. 2016;94:181–188.
15. Cao Y, Pan C, Balter JM, et al. Liver function after irradiation based upon CT portal vein perfusion imaging. *Int J Radiat Oncol Biol Phys*. 2008;70:154–160.
16. Sourbron S, Sommer WH, Reiser MF, Zech CJ. Combined quantification of liver perfusion and function with dynamic gadoxetic acid-enhanced MR imaging. *Radiology*. 2012;263:874–883.
17. Simeth J, Johansson A, Owen D, et al. Quantification of liver function by linearization of a two-compartment model of gadoxetic acid uptake using dynamic contrast-enhanced magnetic resonance imaging. *NMR in Biomedicine*. 31(6):e3913. https://doi.org/10.1002/nbm.3913.
18. Verloh N, Haimerl M, Zeman F, et al. Assessing liver function by liver enhancement during the hepatobiliary phase with Gd-EOB-DTPA-enhanced MRI at 3 Tesla. *Eur Radiol*. 2014;24:1013–1019.
19. Nilsson H, Blomqvist L, Douglas L, Nordell A, Jonas E. Assessment of liver function in primary biliary cirrhosis using Gd-EOB-DTPA-enhanced liver MRI. *HPB*. 2010;12:567–576.

20. Wang H, Feng M, Frey KA, Ten Haken RK, Lawrence TS, Cao Y. Predictive models for regional hepatic function based upon 99mTc-IDA SPECT and local radiation dose for physiological adaptive RT. *Int J Radiat Oncol Biol Phys*. 2013;86:1000–1006.
21. Zou W, Dong L, Kevin Teo BK. Current state of image guidance in radiation oncology: Implications for PTV margin expansion and adaptive therapy. *Sem Radiat Oncol*. 2018;28:238–247.
22. Chin S, Eccles CL, McWilliam A, et al. Magnetic resonance-guided radiation therapy: A review. *J Medl Imag Radiat Oncol*. 2020;64: 163–177.
23. Johnson PJ, Berhane S, Kagebayashi C, et al. Assessment of liver function in patients with hepatocellular carcinoma: A new evidence-based approach-the ALBI grade. *J Clin Oncol*. 2015;33: 550–558.
24. Chandarana H, Block TK, Rosenkrantz AB, et al. Free-breathing radial 3D fat-suppressed T1-weighted gradient echo sequence: A viable alternative for contrast-enhanced liver imaging in patients unable to suspend respiration. *Invest Radiol*. 2011;46:648–653.
25. de Graaf W, Häusler S, Heger M, et al. Transporters involved in the hepatic uptake of 99mTc-mebrofenin and indocyanine green. *J Hepatol*. 2011;54:738–745.
26. Abdalla EK, Denys A, Chevalier P, Nemr RA, Vauthey JN. Total and segmental liver volume variations: Implications for liver surgery. *Surgery*. 2004;135:404–410.
27. Haimerl M, Schlabeck M, Verloh N, et al. Volume-assisted estimation of liver function based on Gd-EOB-DTPA–enhanced MR relaxometry. *Eur Radiol*. 2016;26:1125–1133.
28. Yoneyama T, Fukukura Y, Kamimura K, et al. Efficacy of liver parenchymal enhancement and liver volume to standard liver volume ratio on Gd-EOB-DTPA-enhanced MRI for estimation of liver function. *Eur Radiol*. 2014;24:857–865.
29. Yoon JH, Lee JM, jin Kang H, et al. Quantitative assessment of liver function by using gadoxetic acid–enhanced MRI: Hepatocyte uptake ratio. *Radiology*. 2018;290:125–133.
30. Xu ZY, Liang SX, Zhu J, et al. Prediction of radiation-induced liver disease by Lyman normal-tissue complication probability model in three-dimensional conformal radiation therapy for primary liver carcinoma. *Int J Radiat Oncol Biol Phys*. 2006;65:189–195.
31. Jackson A, Haken RKT, Robertson JM, Kessler ML, Kutcher GJ, Lawrence TS. Analysis of clinical complication data for radiation hepatitis using a parallel architecture model. *Int J Radiat Oncol Biol Phys*. 1995;31:883–891.
32. Price RG, Apisarnthanarax S, Schaub SK, et al. Regional radiation dose-response modeling of functional liver in hepatocellular carcinoma patients with longitudinal sulfur colloid SPECT/CT: A proof of concept. *Int J Radiat Oncol Biol Phys*. 2018;102:1349–1356.
33. Yamada A. Quantitative evaluation of liver function within MR imaging. *OMICS J Radiology*. 2012;1.
34. Yoon JH, Choi JI, Jeong YY, et al. Pre-treatment estimation of future remnant liver function using gadoxetic acid MRI in patients with HCC. *J Hepatol*. 2016;65:1155–1162.
35. Ba-Ssalamah A, Bastati N, Wibmer A, et al. Hepatic gadoxetic acid uptake as a measure of diffuse liver disease: Where are we? *J Magn Res Imag*. 2017;45:646–659.
36. Saito K, Ledsam J, Sourbron S, et al. Measuring hepatic functional reserve using low temporal resolution Gd-EOB-DTPA dynamic contrast-enhanced MRI: A preliminary study comparing galactosyl human serum albumin scintigraphy with indocyanine green retention. *Eur Radiol*. 2014;24:112–119.
37. Leen E, Goldberg JA, Anderson JR, et al. Hepatic perfusion changes in patients with liver metastases: Comparison with those patients with cirrhosis. *Gut*. 1993;34:554–557.